

## **MICROSTRUCTURAL EXAMINATION ON V-4Cr-4Ti RODS AND CREEP TUBES**

- Y. Yan, H. Tsai, and D.L. Smith (Argonne National Laboratory)

### **OBJECTIVE**

The objective of this task is to determine whether the V-4Cr-4Ti bars from the extruded 832665 and swaged 832864 heats are suitable feedstock for the upcoming creep tubing fabrication campaign.

### **SUMMARY**

Extruded V-4Cr-4Ti bar stock from ANL's 500-kg 832665 heat and swaged rod stock from GA's 1000-kg 832864 heat were examined using optical microscopy and transmission electron microscopy to determine whether they are suitable feedstock for the upcoming creep tubing fabrication campaign. To compare microstructure, 832665-heat creep tubing from the last fabrication campaign was also examined. The results of this study show a banded (stringer) structure, consisted of fine Ti-rich particles, exists in both the 832665 and 832864 bars. In the finished creep tubing, remnant of Ti-rich secondary phase particles could also be found although the inhomogeneity is less pronounced than in the feedstock. A homogenization treatment (e.g., annealing at 1200°C for 2 h) may remove the banded structure and this will be tested on small pieces of the 832665 and 832864 bars in the near future.

### **EXPERIMENTAL PROCEDURE**

Specimens were prepared in directions both parallel and perpendicular to the extrusion direction of the bars in order to elucidate the microstructure, particularly the distribution of the banded structure. After mechanical polishing and electropolishing, optical microscopy examinations were conducted to delineate the grain sizes and the microstructural inhomogeneity. Transmission electron microscopy (TEM) studies were carried out to identify the secondary phase particles using a Philips-CM30 microscope, and high resolution electron microscopy (HREM) observations were performed using a JEM-4000EX microscope with a point-to-point resolution of 0.17 nm at Argonne National Laboratory.

### **RESULTS AND DISCUSSION**

There are significant differences in microstructure, including grain sizes between the extruded 832665 and swaged 832864 rods, as shown in the low-magnification micrographs in Figs. 1 and 2. The microstructure of the extruded 832665 material, as shown in Fig. 1(a), consists of an inhomogeneous mixture of small (5-20  $\mu\text{m}$ ) and coarse grains (25-50  $\mu\text{m}$ ). The grains are mostly equiaxed. For the 832864 material, as shown in Fig. 2(a), the grains are elongated parallel to the extrusion direction and the average grain size is larger than that of the 832665 material.

A banded structure parallel to the extrusion direction, as reported by Rowcliffe et al [1], was observed in both materials. The average grain size in the banded region is considerably smaller than that in the un-banded region, particularly for the as-extruded materials from heat no. 832665 (see Fig. 1(a)). The "dark-field" imaging (i.e. using the scattering light illuminating in optical microscopy), as shown in Figs 1(b)-(c) and 2(b)-(c), was used in our examinations to enhance the contrast of the grain boundary structure and the secondary particles. Figs. 1(b) and 2(b) are higher magnification micrographs showing the banded structure in specimens from heat nos. 832665 and 832864, respectively. Detail analyses indicate that the width of the bands and the distances between them are varied from region to region. The typical width of the bands ranges

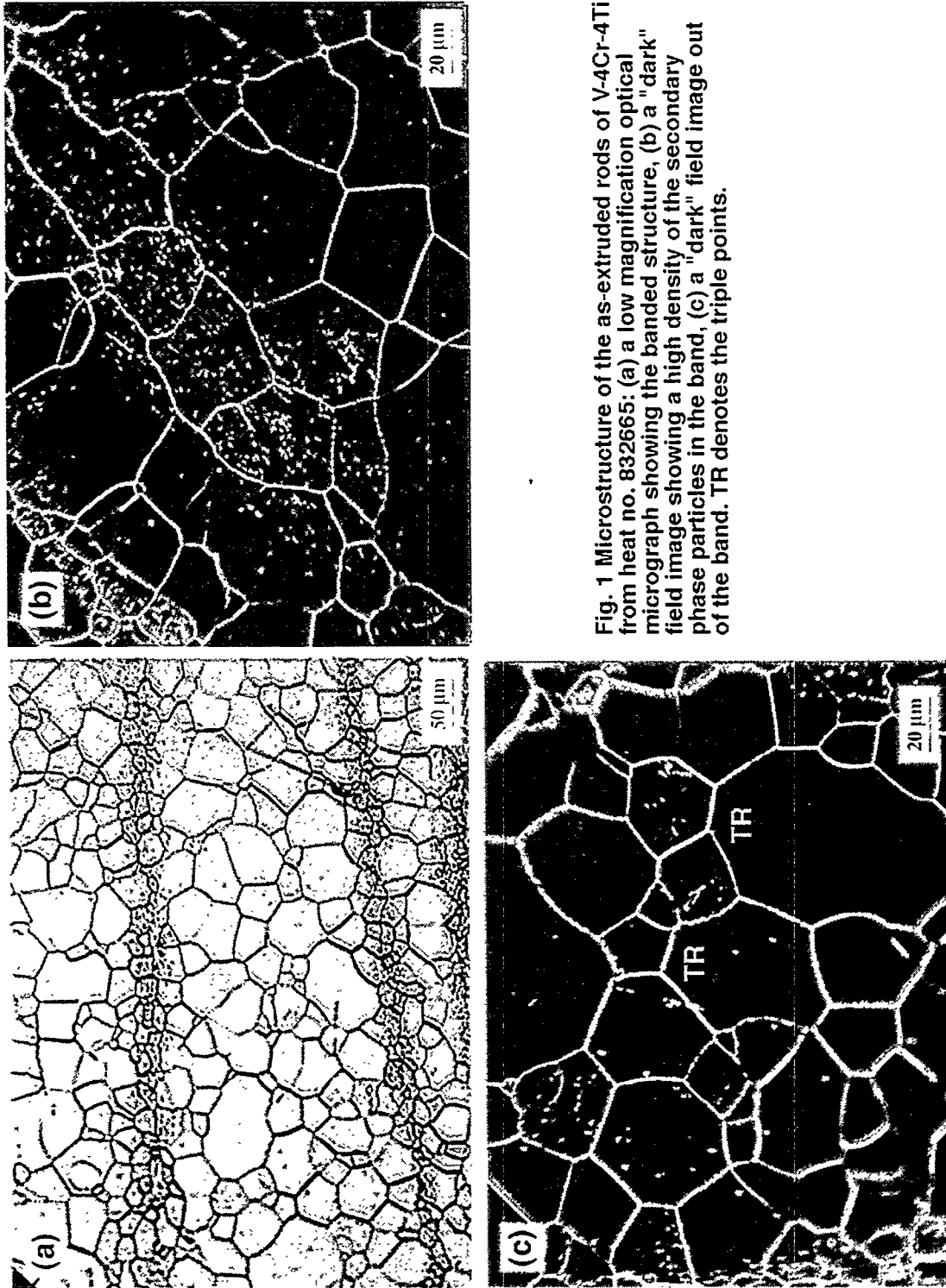


Fig. 1 Microstructure of the as-extruded rods of V-4Cr-4Ti from heat no. 832665: (a) a low magnification optical micrograph showing the banded structure, (b) a "dark" field image showing a high density of the secondary phase particles in the band, (c) a "dark" field image out of the band. TR denotes the triple points.

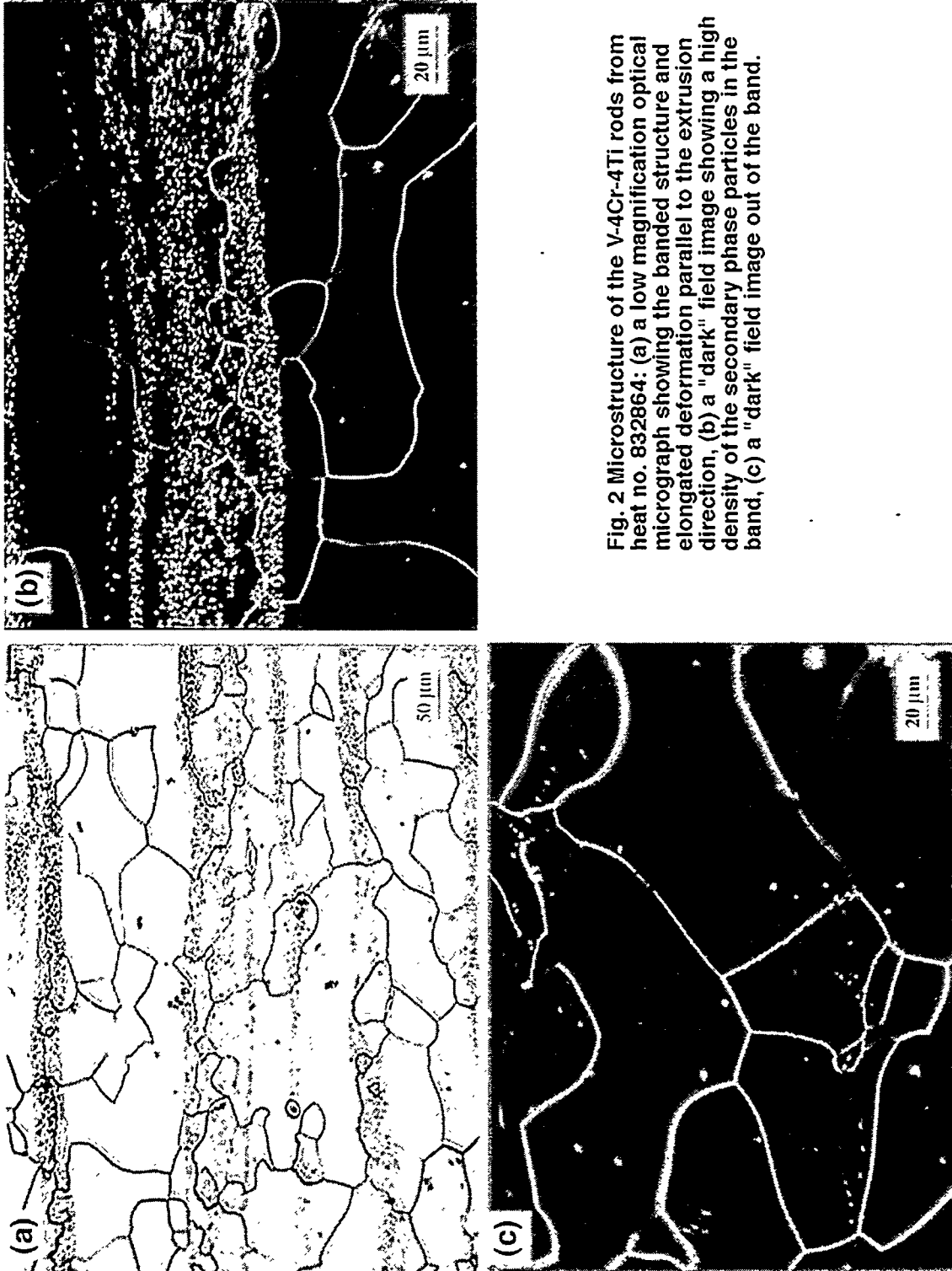


Fig. 2 Microstructure of the V-4Cr-4Ti rods from heat no. 832864: (a) a low magnification optical micrograph showing the banded structure and elongated deformation parallel to the extrusion direction, (b) a "dark" field image showing a high density of the secondary phase particles in the band, (c) a "dark" field image out of the band.

from 25 to 100  $\mu\text{m}$ , and the distances between the bands are  $\approx$  50-150  $\mu\text{m}$  in the specimens examined.

Figs. 1(c) and 2(c) are higher magnification micrographs showing local areas without the banded structure in the extruded 832665 and swaged 832864 materials. There is a strong tendency for grain boundary interfaces to be faceted for as-extruded rods from heat no. 832665 (see Fig. 1(c)). The faceted planes are presumably some low index crystallographic plans, which are usually in favor of formation energy for grain boundaries. At the triple points (marked as TR in Fig. 1(c)) the grain boundaries likely joint together at some special angles, such as  $\sim 90^\circ$ ,  $\sim 120^\circ$ , or  $\sim 135^\circ$ . The tendency to be faceted onto low index plans is decreased for the grain boundaries in the sample from heat no. 832864 due to the deformation induced in swaging processing of round bars from the original materials. It has also been found that the grain sizes are not uniform in the banded areas. Although the average of the grain sizes in the banded area are smaller than that in the un-banded areas, some large grains ( $>30 \mu\text{m}$ ) were also observed occasionally in the banded areas, as shown in Fig. 1(b).

TEM micrograph of Fig. 3(a) shows a secondary phase particle in the 832864 specimen. According to other investigators [1,2], the globular-shaped secondary particles in V-4Cr-4Ti consist of Ti-oxycarbonitrides (Ti-OCN). Our preliminary TEM examinations confirmed the predominant composition of Ti in the secondary phase particles. However, it appears that there is no significant increment of the C and O peaks in the energy dispersive spectrum of the secondary phase particle examined in our sample. A typical energy dispersive spectrum for the impurity phase is shown in Fig. 3(c) and can be compared with the reference spectra obtained from the V-4Cr-4Ti matrix, shown in Fig. 3(b). A more detailed analysis on the secondary phase particles will be conducted in the near future.

Electron diffraction studies did not reveal any preferred orientation of the discrete Ti-rich particle inclusions with respect to the V-4Cr-4Ti matrix. TEM microscopy indicates further that the interface between the V-4Cr-4Ti and secondary phase particles is predominantly non-faceted, as can be seen from Fig. 3(a). High-resolution electron microscopy (HREM) was used to examine the interface structure. The lattice disorder, indicated by the non-uniform contrast in the HREM image (see Fig. 4(a)) of the V-4Cr-4Ti phase around the second phase, was observed, although the spatial distribution of the defects is better viewed at low magnification using the diffraction contrast techniques. The lower magnification using a zone-axis bright-field image shown in Fig. 4(b) reveals the form and distribution of the stress field associated with the secondary phase particle. In the area examined, the dislocations are non-uniformly distributed, with high density near the Ti-based particles. The dislocations appear to extend to distances of up to hundreds of nanometers from the interface of the V-4Cr-4Ti and secondary phase particles.

Limited microstructural characterization on creep tubing from the previous fabrication campaign was conducted to determine whether there are residual inhomogeneity from the feedstock. Optical microscopy, conducted along both longitudinal (see Fig. 5) and transverse (see Fig. 6) directions, shows that the grain sizes are from  $\approx 10$  to 70  $\mu\text{m}$  with elongated deformation parallel to the longitudinal (i.e. drawing) direction (see Fig. 5). The secondary phase particles in the creep tubes distribute more uniformly, as shown in Fig. 5(c), than in the as-extruded feedstock, but the banded structure can still be observed (see Fig. 6(c)).

## FUTURE PLAN

A homogenization treatment (e.g., annealing at 1200°C for 2 h) will be performed on small pieces of the 832665 and 832864 bars, and microstructural examinations on the treated materials will be conducted to determine whether the treatment will re-dissolve the secondary phase particles.

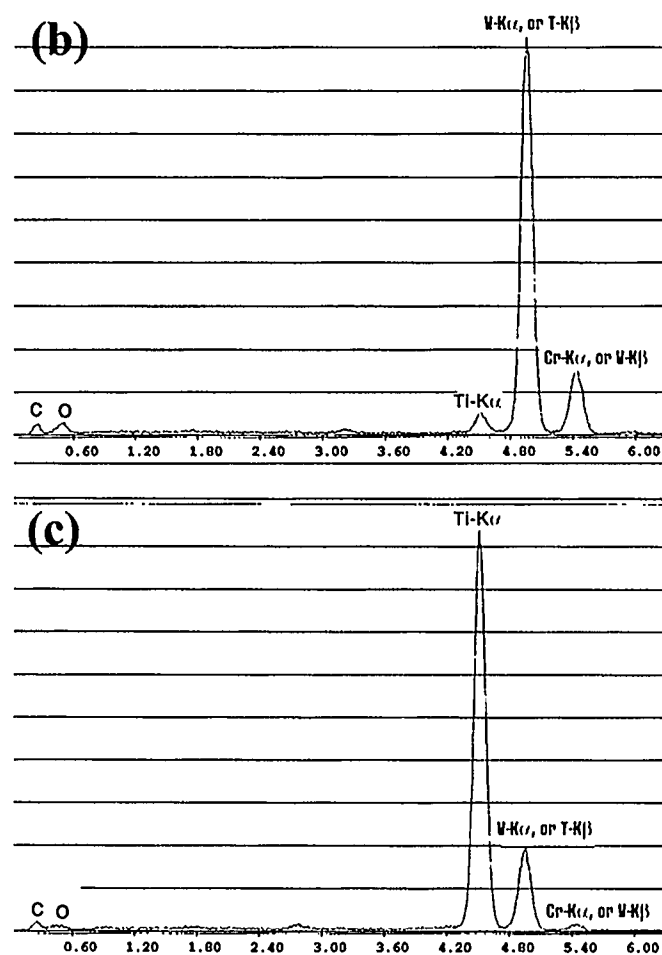


Fig.3 (a) A TEM image showing a secondary phase particle (labeled as B) in the V-4Cr-4Ti rods from heat no. 832864. (b) Energy dispersive spectrum obtained from the V-4Cr-4Ti matrix. (c) Energy dispersive spectrum obtained from the secondary phase particle. Note the lack of noticeable increase in C and O peaks in the spectrum of the particle B.

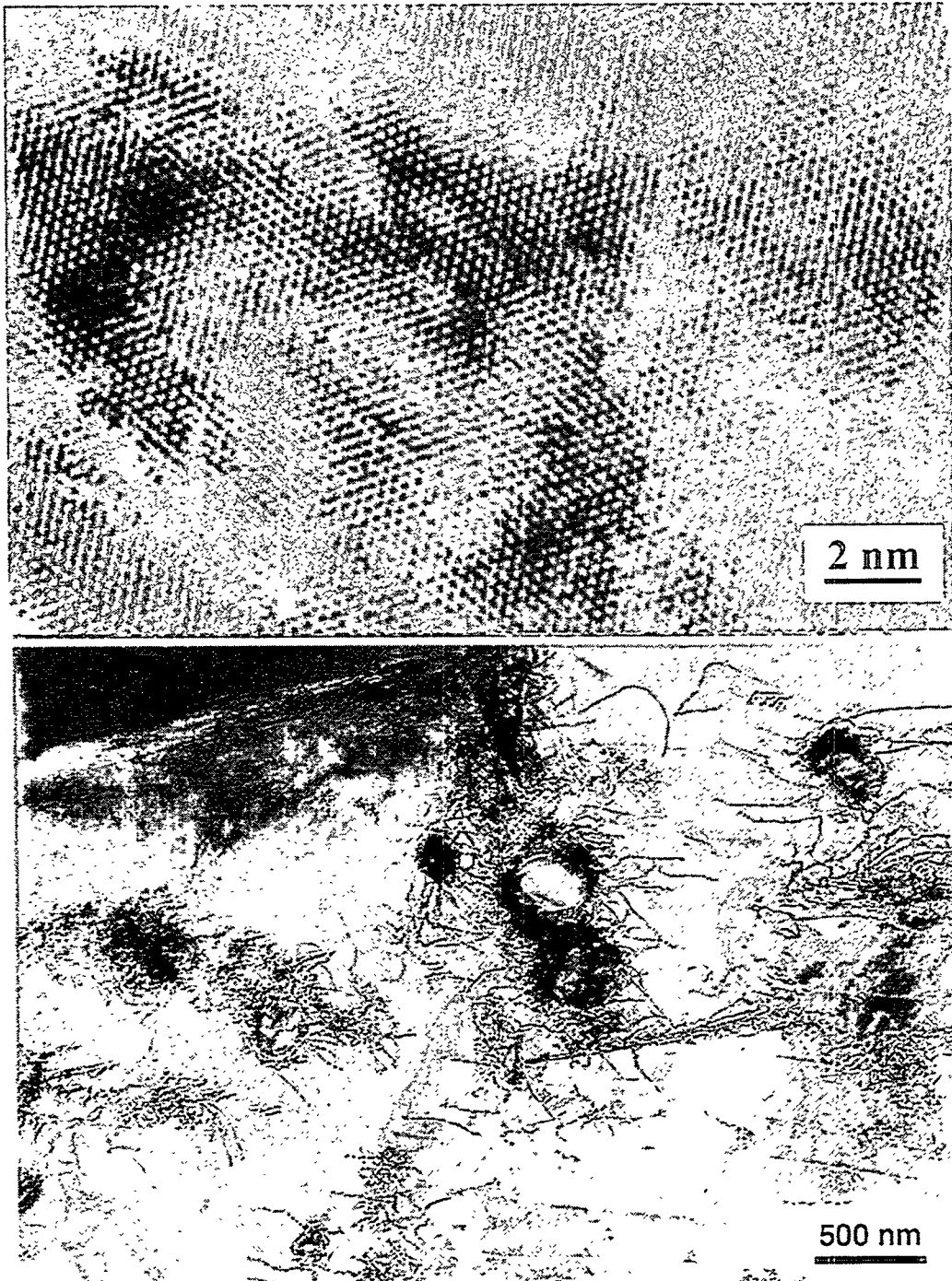


Fig.4 (a) HREM image showing the lattice disorder of the V-4Cr-4Ti phase around the second phase particles. (b) A low magnification TEM micrograph showing the microstructure in the band of the V-4Cr-4Ti rods from heat no. 832864.

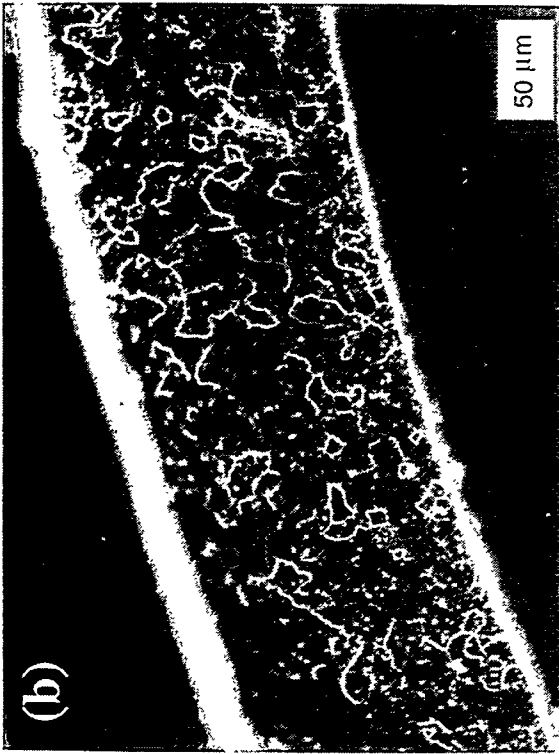


Fig. 5 (a) Optical micrograph of the creep tubing cut along longitudinal direction: (a) a low magnification micrograph showing the grains with elongated deformation parallel to the extrusion direction, (b) a "dark" field image showing the banded structure, (c) a high magnification "dark" field image out of the band.

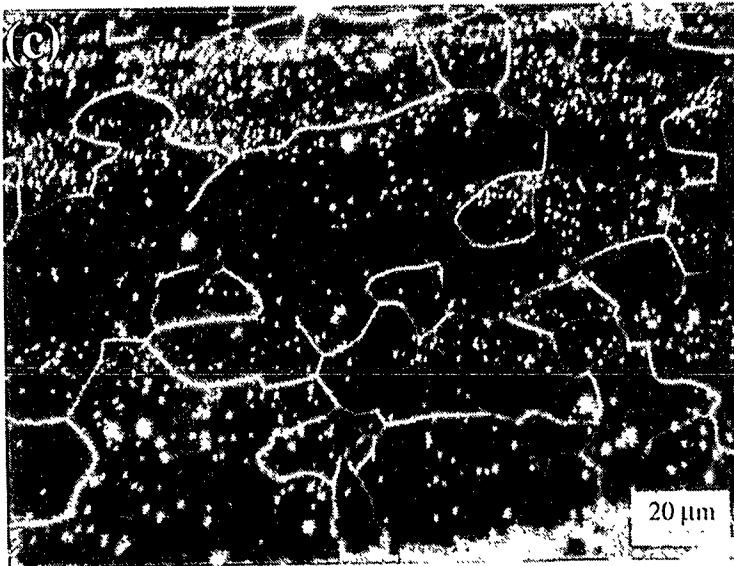
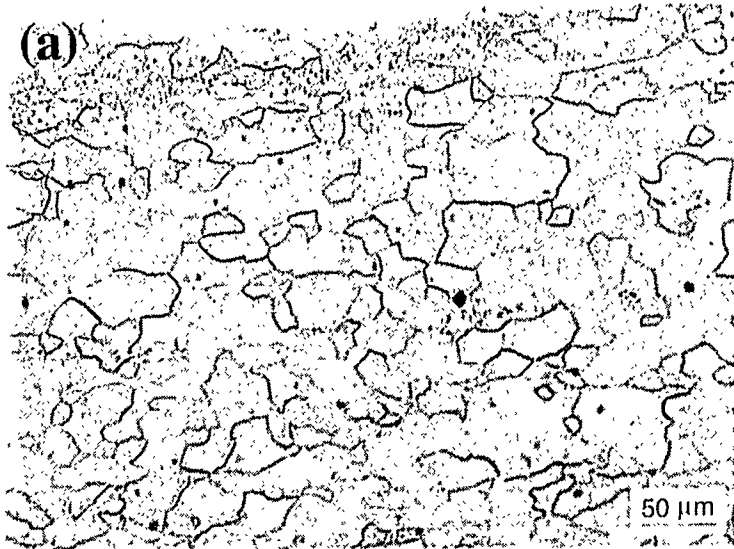


Fig. 6 (a) Optical micrograph of the creep tubing cut along transverse direction: (a) a low magnification optical micrograph and (b) a "dark" field image showing the grain distributions, (c) a high magnification "dark" field image showing a local banded structure.

**ACKNOWLEDGEMENTS**

We are grateful to Dr. R. Cook and Mr. B. Kestel for helping with the sample preparing. We also acknowledge the support of Dr. M.A. Kirk of Electron Microscopy Center, Argonne National Laboratory, for the provision of laboratory facilities.

**REFERENCES**

1. F. Rowcliffe and D. T. Hoelzer, Fusion Materials Semiannual Progress Report, DOE/ER-0313/25, December 1998, pp42-58.
2. D. T. Hoelzer, Fusion Materials Semiannual Progress Report, DOE/ER-0313/25, December 1998, pp. 59-63.